JRAEE

Journal of Robotics, Automation, and Electronics Engineering
Vol. 2, No. 1, 2024, pp. 30-38
e-ISSN 3025-3780
https://journal.uny.ac.id/publications/jraee

Rotman Lens Size Reduction by Using Same-Size Double Rectangular Defected Ground Structures (DGSs) Method or Same-Size Double Rectangular Slots Method

Rizky Hidayat Prasetyo[a,1,*], Eko Tjipto Rahardjo[b]

[a] Universitas Negeri Yogyakarta
[b] Universitas Indonesia
[1] rizkyhidayat@uny.ac.id
[*] Corresponding Author

ARTICLE INFO

Article History
Received 20 Jan. 2024
Revised 15 Mar. 2024
Accepted 5 May 2024

Keywords
Rotman Lens;
Multi-beamforming;
Array;
Antenna.

ABSTRACT

The need for dedicated communication keeps increasing. A technique to realize that is by using multibeam radiation. A Beamforming Network (BFN) is required to enable multibeam capability in array antennas. This study uses the Rotman Lens as BFN in the frequency of S-Band. The common problem with using Rotman Lens is that its conventional design size is quite large, mainly due to its transition leg ports. Transition leg ports are important to ensure the matching impedance between the lens and the array antenna ports the lens and the beam ports or the lens and the dummy port. The goal of this study is to reduce the size of Rotman lens transition legs by implementing simple and uniform size of slots or Defected Ground Structures (DGSs) methods for the ports of the Rotman Lens BFN. The method can minimize the length of the transition leg and allow the BFN to operate efficiently. The results revealed that the use of the same double-rectangular DGS technique and the same double-rectangular slots in ports can reduce the size of the Rotman lens. Compared to the conventional methods, the proposed method can reduce the size to almost 85 percent from its original size for this S-Band implementation. The other performances of the BFN, besides the size reduction, are not degraded by implementing the proposed methods.

Kebutuhan akan komunikasi khusus terus meningkat. Salah satu teknik untuk mewujudkan hal tersebut adalah dengan membuat pola radiasi banyak arah. Beamforming Network (BFN) diperlukan untuk membuat pola radiasi banyak arah pada antena array. Penelitian ini menggunakan Rotman Lens sebagai BFN pada frekuensi S-Band. Masalah umum dalam menggunakan Rotman Lens adalah ukuran desain konvensionalnya yang cukup besar, terutama karena port kaki transisinya. Port kaki transisi penting untuk memastikan kesesuaian impedansi antara lensa dengan port antena atau lensa dengan port beam atau lensa dengan port dummy. Tujuan dari penelitian ini adalah untuk mengurangi ukuran kaki transisi Rotman Lens dengan menerapkan metode yang sederhana dan ukuran seragam yaitu dengan slot atau Defected Ground Structure (DGS) untuk port kaki transisi Rotman Lens. Metode ini dapat mengurangi panjang kaki transisi dan memungkinkan BFN beroperasi secara efisien.

Hasil simulasi maupun pengukuran menunjukkan bahwa penggunaan teknik DGS persegi panjang ganda maupun slot persegi panjang ganda dengan ukuran sama pada port dapat memperkecil ukuran lensa Rotman. Dibandingkan dengan metode konvensional, metode yang diusulkan dapat memperkecil ukuran hingga hampir 85 persen dari ukuran aslinya pada implementasi di frekuensi S-Band. Kinerja lainnya, selain pengurangan ukuran, tidak terdegradasi dengan diterapkannya metode yang diusulkan.

1. Introduction

In recent decades, multi-beamforming antenna systems have attracted increasing widespread attention. They have been widely used in many fields, such as autonomous vehicles, radar, and communications. In the development, three different types of beamforming networks can be used to enable the multibeam operation. They are digital, analog, and hybrid BFN. Digital (and also hybrid) BFN is still costly. For the low-cost BFN, analog BFN is usually used.

There are several types of analog BFN. The main idea for this is to use a time or phase delay mechanism to create radiation in certain directions. By using microstrip substrate, [1] [2] used the Butler matrix concept, [3] [4] used the Blass matrix concept, [5] [6] [7] used the Nolen matrix concept as their BFN. Meanwhile [8] [9] [10] [11] using Lens concept as their BFN. Another researcher also used biconical [12], strip delay lines [13], and meta surface [14] to form multibeam characteristics.

One of the interesting BFNs is the Rotman Lens. It has wideband resonant frequency characteristics, a relatively more flexible phase differentiating design, and relatively low complexity regarding the number of ports that can be assigned. But, the Rotman Lens structure is usually quite large, it is about 6λ [15]. The large conventional Rotman lens size is mainly due to its transition leg ports. Some researchers have tried to tackle this issue. [16] used Klopfenstein's taper lines concept. [17] used single energy distribution slots with different sizes in each port. [18] used dual-crescent-dumble-like DGS structures with different sizes in each beam port. And [15] used the meta-transmission line concept.

This study would like to reduce the size of Rotman lens transition legs by implementing simple and uniform size of slots or Defected Ground Structures (DGSs) methods for all the ports of the Rotman Lens in S-band frequency. The contribution of the research is that this research successfully reduced the size of the Rotman Lens by using the same-size double-rectangular DGS technique or by using the same-size double-rectangular slots in all ports. This technique also reduces the iterations that often have to be done a lot.

The rest of the paper is as follows. Chapter 2 will explain the basics of Rotman Lens, Chapter 3 will explain the reduction method, Chapter 4 will discuss the results of the reduction, and Chapter 5 will conclude the research.

2. Basic of Rotman Lens

The structure of the Rotman lens is composed of a pair of metal plates that are aligned parallel to each other. In its early development, the space between the two metal plates was left to be filled with air, but in more recent advancements, it is filled with a certain dielectric substrate. The size of the Rotman lens depends on the permittivity of the substrate. A greater permittivity results in a smaller size for the Rotman lens.

Rotman Lens has three main parts. The first part is array ports, where the lens is connected to the array antenna. The second part is beam ports where excitation ports are connected to (when used as a transmitter) or signal is gathered (when used as a receiver). The last part is dummy ports where

ISSN 3025-3780 (online)
ISSN 3025-4590 (printed)

internal reflections are absorbed.

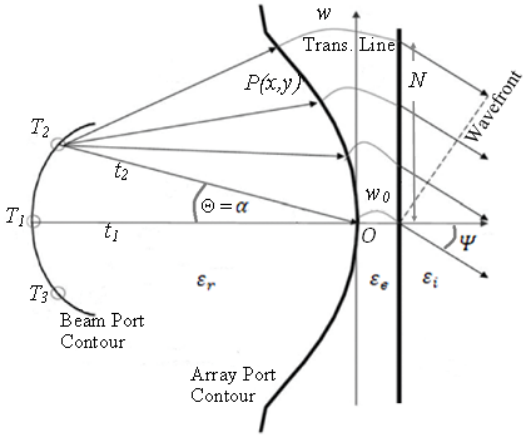

Fig. 1. Basic Geometry of Rotman Lens

In this paper, Trifocal formulations are utilized to design the Rotman Lens, like in [19]. First of all, three points should be determined from the origin point (O) with the radius of t1, t2, and t3, where t2 has the same length as t3. Then, the trifocal points T1, T2, and T3. Here we get that t2 is symmetrical with t1. After that, we have the following equations to determine the position of the array port contour.

$$T_1P\sqrt{\varepsilon_r} + W\sqrt{\varepsilon_e} = t_1\sqrt{\varepsilon_r} + W_0\sqrt{\varepsilon_e} \quad (1)$$

$$T_2P\sqrt{\varepsilon_r} + W\sqrt{\varepsilon_e} + N\sqrt{\varepsilon_i}sin \propto = t_2\sqrt{\varepsilon_r} + W_0\sqrt{\varepsilon_e} \quad (2)$$

$$T_3P\sqrt{\varepsilon_r} + W\sqrt{\varepsilon_e} - N\sqrt{\varepsilon_i}sin \propto = t_2\sqrt{\varepsilon_r} + W_0\sqrt{\varepsilon_e} \quad (3)$$

When substrate with a dielectric constant of ε_r is in the lens, substrate with the dielectric constant of ε_e is in the transmission lines, and substrate with a dielectric constant of ε_i is in the antenna; some more equations should be used

$$w = \frac{\sqrt{\varepsilon_e}}{\sqrt{\varepsilon_r}} \frac{-b \pm \sqrt{b^2 - 4ac}}{2a} \quad (4)$$

$$x = \frac{\varepsilon_i N^2 sin^2\Psi}{2\,\varepsilon_r\,(\beta cos\alpha - 1)} + \frac{(1-\beta)w}{\beta cos\alpha - 1}\sqrt{\frac{\varepsilon_e}{\varepsilon_r}} \quad (5)$$

$$y = \sqrt{\frac{\varepsilon_e}{\varepsilon_r}} \frac{N\,sin^2\Psi}{t_1\,sin \propto}\left(1 - \frac{w}{\beta}\sqrt{\frac{\varepsilon_e}{\varepsilon_r}}\right) \quad (6)$$

Where

$$a = 1 - \left(\frac{1-\beta}{1-\beta C}\right)^2 - \frac{\zeta^2}{\beta^2}\frac{\varepsilon_e}{\varepsilon_r} \quad (7)$$

$$b = -2 + \frac{2\zeta^2}{\beta}\frac{\varepsilon_i}{\varepsilon_r} + 2\left(\frac{1-\beta}{1-\beta C}\right) - \frac{\zeta^2 s^2(1-\beta)}{(1-\beta C)^2}\frac{\varepsilon_i}{\varepsilon_r} \quad (8)$$

$$c = \left(-\zeta^2 + \frac{\zeta^2 S^2}{(1-\beta C)} - \frac{\zeta^2 S^4}{4(1-\beta C)}\right)\frac{\varepsilon_i}{\varepsilon_r} \quad (9)$$

$$\beta = \frac{t_2}{t_1} \quad (10)$$

$$\zeta = \frac{N\,sin\Psi}{t_1\,sin\alpha} \quad (11)$$

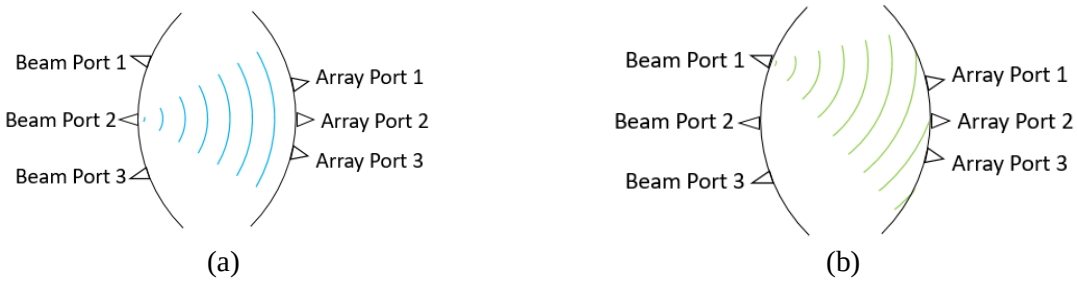

Fig. 2. (a) Phase front pattern when Beam Port 2 activated, while (b) Phase front pattern when Beam Port 1 activated

It is assumed that the array ports will receive the appropriate phases of the incoming waves based on the equations shown in Figure 2. The blue curves in Figure 2 (a) show the phase front pattern of the port with the excited center beam. It is possible to deduce that the array ports will get the same phase and will make radiation that is perpendicular to the plane.

The green curves in Fig. 2 (b) show the phase front arrangement of the port when it is excited. The phase differences in the neighboring array ports will also affect the direction of the radiation of the antenna. This is because the linearities of the successive array port's phase difference will shift the beam's direction not to be perpendicular to the plane.

When two array ports are excited at the same time, there will be two radiation patterns produced by the array antenna. This means that through a Rotman lens, multi-beam operation can be achieved.

3. Proposed Method for Reducing Rotman Lens Size

In this research, the Rotman Lens is designed to work in S-band frequency. The substrate that is being used for all ports and lens structures is FR-4 whose dielectric constant is 4.3. The number of the beam port is five (it is depicted in Fig 3 with ports 1,2,3,8 and 9; port 1 is symmetrical with port 9) to make five directional radiation patterns. While the number of the array port is six (ports 4,5,6,10,11, and 12). Array antenna elements used are also six. The space between array antenna elements is arranged to be half of the wavelength. The number of the dummy ports is two (ports 7 and 13).

There will be 3 Rotman structures shown here. They are the conventional one which employs a long transition leg, the reduced Rotman lens by using the DGS technique, and the reduced one by using the slot technique. All those 3 structures should qualify the same design parameter shown in Table 1 below.

Table 1. Rotman Lens Design Parameters

Parameter	Value
Frequency	S-Band
Number of Beam Ports	5
Number of Array Ports	6
Spacing Between Array	λ/2
α	36 °
β	0.9
ζ	1.1
Bandwidth	100 MHz
Return Loss	≤ -9,54 dB
Designated Beam Directions	±36, ±18, 0

ISSN 3025-3780 (online)
ISSN 3025-4590 (printed)

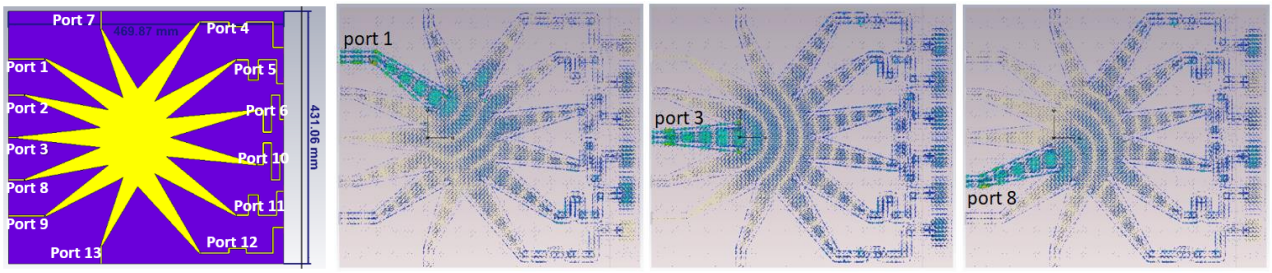

Fig. 3. Conventional Rotman Model and Its Surface Current Profile when Port 1, 3, and 8 are excited

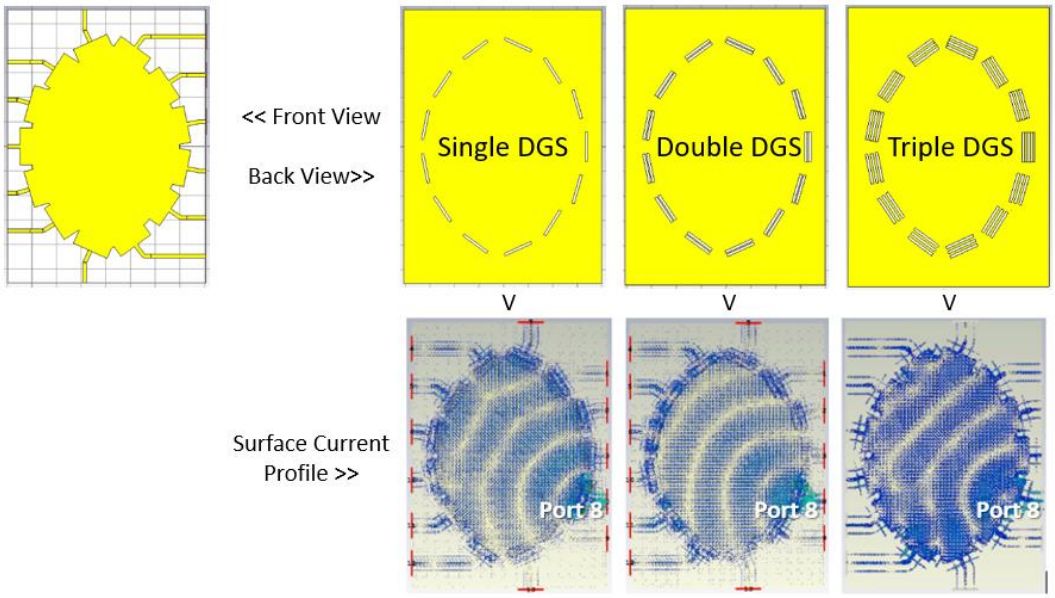

Fig. 4. Reduced Rotman Lens Models by DGS Technique and Its Surface Current Pattern when Port 8 is excited

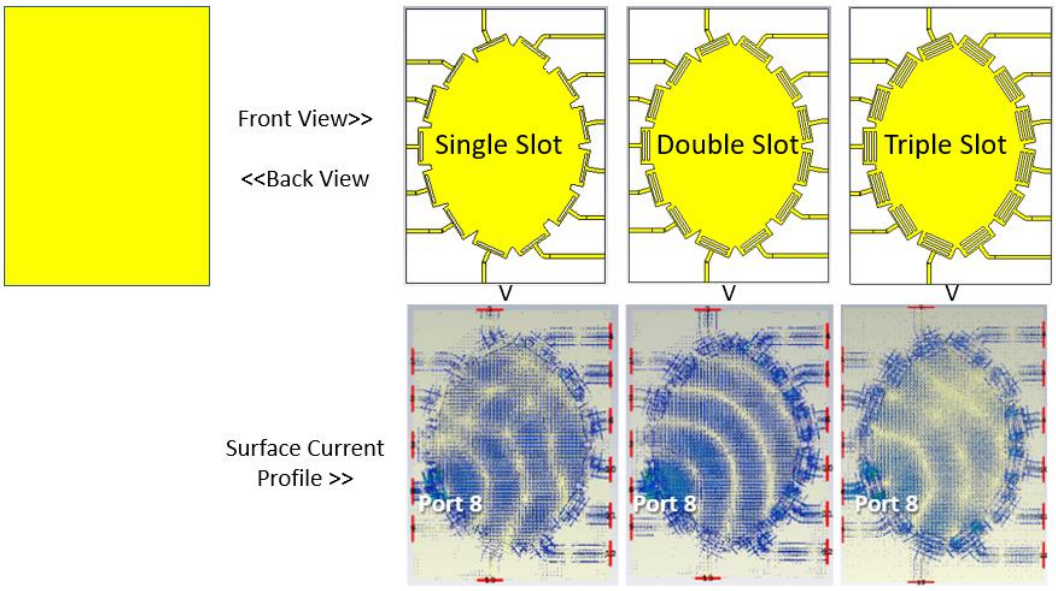

Fig. 5. Reduced Rotman Lens Models by Slot Technique and Its Surface Current Pattern when Port 8 is excited

3.1 Conventional Method

In this conventional method, the length of the leg transition is quite long due to the flare angle. The flare angle should be less than 12.5 degrees. This flare angle guarantees a smooth impedance continuity transition so that return loss can be low. The model built by this conventional model can be seen in Fig. 3. The resulting surface currents are also smooth for all time. It indicates that the impedance matching is good and impedance discontinuity is low.

3.2 Reduction by DGS Method

The long transition legs of the Rotman lens were truncated and DGS was applied to each port. Before determining what shape could reduce the Rotman lens well, investigating the characteristics of a simple DGS shape is needed. Parametric studies were conducted to examine the effect of the length and width of a single rectangular DGS on the return loss of each port. It was found that a single DGS structure will resonate in various frequencies in each port. The longer the length, the resonant frequency will shift to the higher frequency. The wider the width, the resonant frequency will shift to the higher frequency as well (except port number 2) with better return loss value. However, there had not been any single structure in all ports to resonate in S-Band.

Parametric studies were continued with dumbell structure. Dumbell structure was chosen because many researchers in antenna and or microwave devices showed good results/performances by employing this kind of structure. It investigated the effect of the length and the width of the head of the dumbell. The longer and wider of the head will result in a higher return loss.

Because there was no fit result, the study continued to employ two identical rectangular DGSs. It was hoped to create mutual resonant frequency so that the bandwidth is broad. It turned out that the idea was fruitful, the bandwidth became broad and it covered the 2.45 GHz ISM band as well.

Optimization was continued by using 3 identical DGSs. However, the results showed that the frequency was shifted to the lower frequency.

Fig. 4 shows the structure of the reduced Rotman lens by the DGS technique. From the surface current profile, it can be seen that the smooth current flow is only in double DGS whose return loss is low.

3.3 Reduction by Slot Method

The same as reduction by the DGS technique, before determining what shape could reduce the Rotman lens well, investigating the characteristics of a simple slot shape is needed. Parametric studies were also conducted to examine the effect of the length, width, and area of rectangular slots on the return loss of each port.

In the slot technique, it was also found that a single slot structure will resonate in various frequencies in one port and another. The longer the length of the slot, the resonant frequency will shift to the higher frequency. The wider the width, the resonant frequency will shift to the lower frequency. The larger area of the slot can’t be concluded. However, there was not been any single structure in all ports to resonate in the S-Band.

Because there was no fit result, the study continued to employ two identical rectangular slots. As in double DGS, it was hoped to create mutual resonant frequency so that the bandwidth is broad as well. It turned out that the idea was fruitful as well, the bandwidth became broad and it also covered the S-band including the 2.45 GHz ISM band.

Optimization was continued by using 3 identical slots. However, the results showed that the frequency was shifted to the lower frequency, as in the DGS technique.

Fig. 5 shows the structure of the reduced Rotman lens by slot technique. From the surface current profile, it can be seen that the smooth current flow is only in a double slot whose return loss is low, as in DGS. When there are 1 or 3 slots, the surface current flow is not smooth because the return loss is high. The phase front pattern is degraded when 1 or 3 slots are employed.

ISSN 3025-3780 (online)
ISSN 3025-4590 (printed)

Table 2. Performance Comparison Among Conventional, double DGS, and Double Slot

	Conventional			Double DGS			Double Slot		
	Dir.	***Gain***	***SLL***	***Dir.***	***Gain***	***SLL***	***Dir.***	***Gain***	***SLL***
Port 1	35	0.5	-5.2	37	1.42	-8.8	36	2.26	-10.9
Port 2	18	0.92	-6.5	18	3.47	-9.8	19	3.37	-11.3
Port 3	0	1.45	-10.5	0	5.37	-11.6	0	4.67	-12.8
Average		0.96	-7.40		3.42	-10.07		3.43	-11.67

4. Results and Discussion

The performance of the reduced structure by double DGS or double slots is compared to the performance of the conventional Rotman model. After getting the appropriate technique, the reduced Rotman lens is integrated into the array antenna with transmission line adjustment. After that, a far field simulation is conducted to get the radiation pattern including the direction of the beam, gain, and sidelobe level.

Table 2. shows the comparison of the performance of the Rotman lens made by a conventional method, the reduced by Double DGS Technique, and the reduced by Double Slot Technique. There are no significant differences in terms of direction of the beam. While for the gain, the gain of the conventional is lower than the reduced, it is possible because the loss in the conventional is higher for its large structure. The sidelobe level is also lower in the conventional than the reduced, this could happen because the large structure of the conventional affects the radiation of the antenna for its nearfield is also larger.

To validate the result, fabrication and measurement were conducted. The one which is fabricated is the reduced with double slot. The bandwidth is quite similar in ports 1, 2, 8, and 9. Port 1, 2, 8, and 9 reach wide bandwidth characteristics. The port 3 shows multiband characteristic. This happens because port 3 receives more reflection for its design. Fig. 6 shows the measured Return Loss profiles of ports 1, 2, 3, 8, and 9 in the 2.3-2.6 GHz range.

Radiation pattern measurement is done in one full rotation for port 3, and -60 to 60 degrees for other ports. The simulations and the measurements show quite similar results. The measured gain and SLL are also similar to the simulation. The maximum difference is 2 dB. The multi-beam radiation patterns can be seen in Fig. 7. They indicate that the design with the new method is proper.

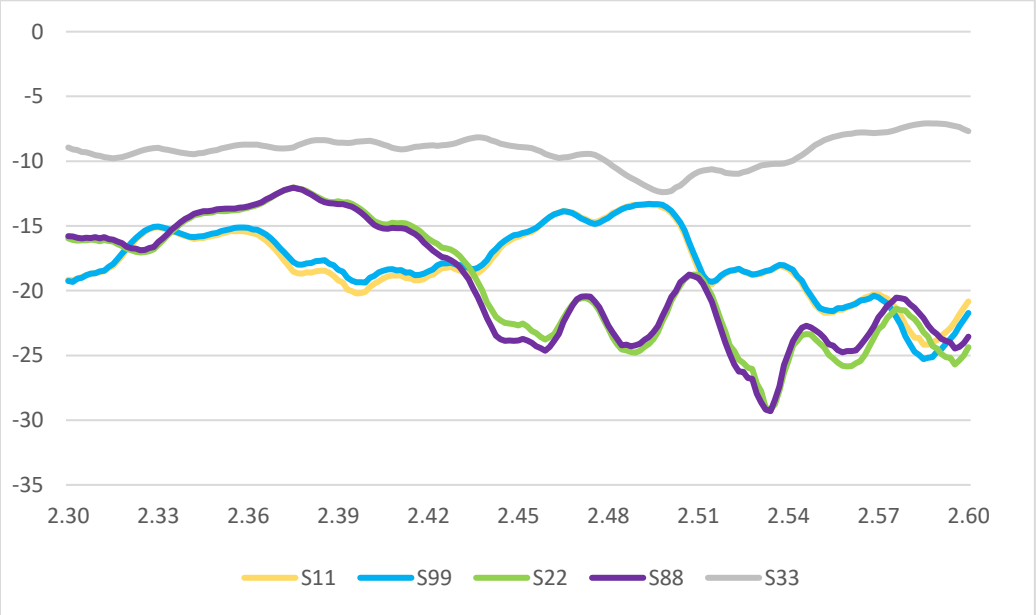

Fig. 6. Measured Return Loss Profiles of Port 1, 2, 3, 8, and 9 in 2.3-2.6 GHz Range

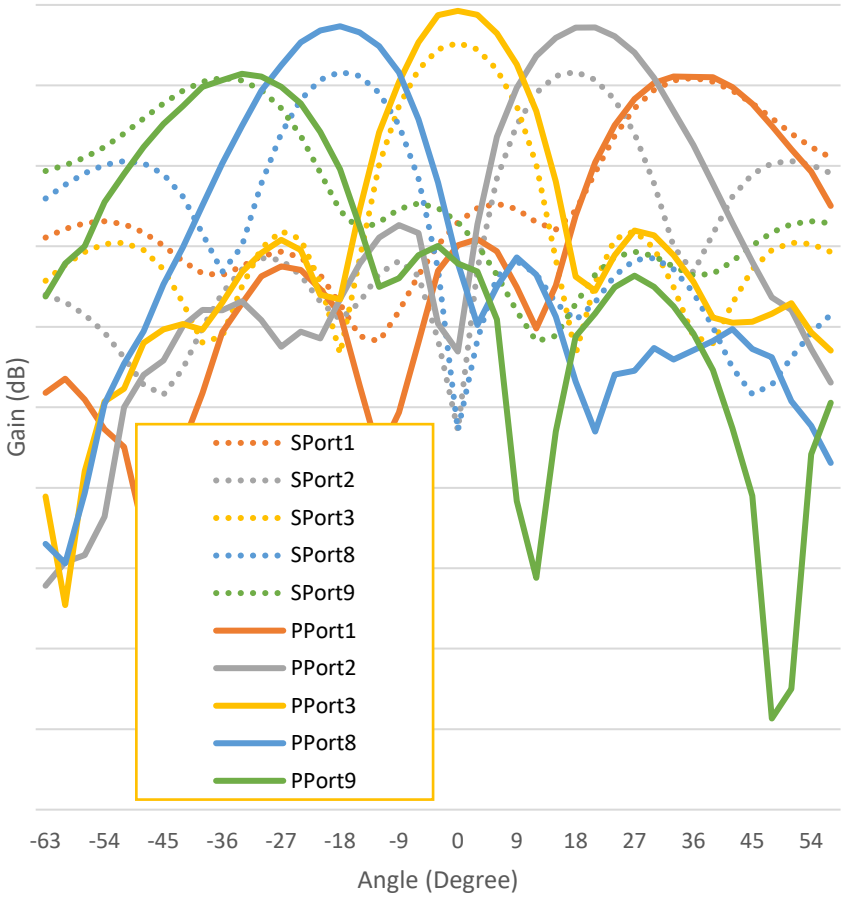

Fig. 7. Radiation Pattern of All Beam Port (f : 2.5 GHz) (dash line [SPort*x*] is simulation result, connected line [PPort*x*] is measurement result)

5. Conclusion

In this research, the miniaturization of Rotman by utilizing the DGS and slots method has been successfully designed, fabricated, and measured in S-Band frequency. The development of new techniques, namely the same-size double rectangular DGS technique and the same-size double rectangular slot, has been proven to decrease the size of the Rotman lens to become about 15 percent from its origin compared to the size of conventional design. This also means simpler design and fewer iterations can be achieved compared to the previous studies. No significant degradation of the performances resulted from the reduction countered as well.

References

[1] B. Shallah et al., "A Miniaturized Metamaterial-Based Dual-Band 4×4 Butler Matrix With Enhanced Frequency Ratio for Sub-6 GHz 5G Applications," in IEEE Access, vol. 12, pp. 32320-32333, 2024, doi: 10.1109/ACCESS.2024.3371027.

[2] Q. Yang et al., "A Low Complexity 16×16 Butler Matrix Design Using Eight-Port Hybrids," in IEEE Access, vol. 7, pp. 177864-177873, 2019, doi: 10.1109/ACCESS.2019.2958739.

[3] G. Buttazzoni et al., "A Simple Blass Matrix Design Strategy for Multibeam Arbitrary Linear Antenna Arrays," in IEEE Transactions on Antennas and Propagation, vol. 71, no. 11, pp. 8514-8524, Nov. 2023, doi: 10.1109/TAP.2023.3310148.

[4] D. I. Lialios, C. L. Zekios and S. V. Georgakopoulos, "A Compact mmWave SIW Blass Matrix," 2021 IEEE International Symposium on Antennas and Propagation and USNC-URSI Radio Science Meeting

ISSN 3025-3780 (online)
ISSN 3025-4590 (printed)

(APS/URSI), Singapore, Singapore, 2021, pp. 961-962, doi: 10.1109/APS/URSI47566.2021.9703822.

[5] Y. Xu, H. Zhu and Y. J. Guo, "Compact Wideband 3 × 3 Nolen Matrix With Couplers Integrated With Phase Shifters," in IEEE Microwave and Wireless Technology Letters, vol. 34, no. 2, pp. 159-162, Feb. 2024, doi: 10.1109/LMWT.2023.3341791.

[6] H. Ren, H. Zhang, Y. Jin, Y. Gu and B. Arigong, "A Novel 2-D 3×3 Nolen Matrix for 2-D Beamforming Applications," in IEEE Transactions on Microwave Theory and Techniques, vol. 67, no. 11, pp. 4622-4631, Nov. 2019, doi: 10.1109/TMTT.2019.2917211.

[7] T. Djerafi, N. J. G. Fonseca and K. Wu, "Broadband Substrate Integrated Waveguide 4$\,\times\,$4 Nolen Matrix Based on Coupler Delay Compensation," in IEEE Transactions on Microwave Theory and Techniques, vol. 59, no. 7, pp. 1740-1745, July 2011, doi: 10.1109/TMTT.2011.2142320.

[8] K. Trzebiatowski, W. Kalista, M. Rzymowski, Ł. Kulas and K. Nyka, "Multibeam Antenna for Ka-Band CubeSat Connectivity Using 3-D Printed Lens and Antenna Array," in IEEE Antennas and Wireless Propagation Letters, vol. 21, no. 11, pp. 2244-2248, Nov. 2022, doi: 10.1109/LAWP.2022.3189073.

[9] M. Muhsin, K. Kamardin, Y. Yamada, Y. Sugimoto and K. Sakakibara, "Best Feed Positions and Radiation Patterns of Typical Multibeam Dielectric Lens Antenna," in IEEE Access, vol. 12, pp. 10497-10511, 2024, doi: 10.1109/ACCESS.2024.3352132.

[10] P. Castillo-Tapia et al., "Two-Dimensional Beam Steering Using a Stacked Modulated Geodesic Luneburg Lens Array Antenna for 5G and Beyond," in IEEE Transactions on Antennas and Propagation, vol. 71, no. 1, pp. 487-496, Jan. 2023, doi: 10.1109/TAP.2022.3217175.

[11] A. M. A. Najafabadi, F. A. Ghani, M. B. Ozdemir and I. Tekin, "5G Antenna Array Fed by a Microstrip Rotman Lens," 2023 IEEE-APS Topical Conference on Antennas and Propagation in Wireless Communications (APWC), Venice, Italy, 2023, pp. 141-141

[12] M. Zoghi, F. Hodjatkashani and M. E. Lajevardi, "An Ultra-Wideband Ridged Biconical Multibeam Antenna," in IEEE Access, vol. 11, pp. 58037-58045, 2023, doi: 10.1109/ACCESS.2023.3282871.

[13] A. M. H. Nasr and K. Sarabandi, "A Low-Cost Millimeter-Wave 5G V2X Multi-Beam Dual-Polarized Windshield Antenna," in IEEE Open Journal of Antennas and Propagation, vol. 3, pp. 1313-1323, 2022, doi: 10.1109/OJAP.2022.3224807.

[14] L. Stefanini et al., "Multibeam Scanning Antenna System Based on Beamforming Metasurface for Fast 5G NR Initial Access," in IEEE Access, vol. 10, pp. 65982-65995, 2022, doi: 10.1109/ACCESS.2022.3183754.

[15] B. G. Kashyap, R. Diaz and G. C. Trichopoulos, "Toward Hyper-Compact Rotman Lenses: Meta-Transmission Line Design and Characterization," 2023 IEEE International Symposium on Antennas and Propagation and USNC-URSI Radio Science Meeting (USNC-URSI), Portland, OR, USA, 2023, pp. 797-798, doi: 10.1109/USNC-URSI52151.2023.10238073.

[16] R. K. Arya et al., "Compact Rotman Lens Design using Klopfenstein Taper Lines," 2022 IEEE 10th Asia-Pacific Conference on Antennas and Propagation (APCAP), Xiamen, China, 2022, pp. 1-2, doi: 10.1109/APCAP56600.2022.10069996.

[17] Q. Liang, B. Sun, G. Zhou, J. Zhao and G. Zhang, "Design of Compact Rotman Lens Using Truncated Ports With Energy Distribution Slots," in IEEE Access, vol. 7, pp. 120766-120773, 2019, doi: 10.1109/ACCESS.2019.2925000.

[18] M. K. Al-Obaidi, E. Mohd, N. Abdullah, and S. H. Dahlan, “A new approach for impedance matching rotman lens using defected ground structure,” Bulletin of Electrical Engineering and Informatics, vol. 9, no. 2, pp. 626–634, Apr. 2020, doi: 10.11591/EEI.V9I2.1850.

[19] H. -T. Chou and D. Torrungrueng, "Development of 2-D Generalized Tri-Focal Rotman Lens Beamforming Network to Excite Conformal Phased Arrays of Antennas for General Near/Far-Field Multi-Beam Radiations," in IEEE Access, vol. 9, pp. 49176-49188, 2021, doi: 10.1109/ACCESS.2021.3068831.